

# Thermodynamic and kinetic factors in the hydrothermal synthesis of hybrid frameworks: zinc 4-cyclohexene-1,2-dicarboxylates†

Clare Lee,<sup>ab</sup> Caroline Mellot-Draznieks,<sup>c</sup> Ben Slater,<sup>c</sup> G. Wu,<sup>d</sup> William T. A. Harrison,<sup>b</sup> C. N. R. Rao<sup>e</sup> and Anthony K. Cheetham<sup>\*a</sup>

Received (in Cambridge, MA, USA) 21st March 2006, Accepted 17th May 2006

First published as an Advance Article on the web 31st May 2006

DOI: 10.1039/b603512d

Experimental and computational studies indicate that the formation of a series of zinc 4-cyclohexene-1,2-dicarboxylates takes place under thermodynamic rather than kinetic control.

There has been extensive work in recent years on the synthesis and characterization of hybrid inorganic–organic framework materials based on metal carboxylates.<sup>1</sup> These syntheses have yielded an extraordinary diversity of products<sup>2–4</sup> depending on parameters such as the reaction temperature, time, the concentration of starting materials and the solvent. A systematic study on cobalt succinates<sup>5</sup> revealed the most important variable to be the reaction temperature, suggesting that the products form under local thermodynamic control. Here, we report three new hybrid materials resulting from reactions of zinc oxide with 4-cyclohexene *cis*-1,2-dicarboxylic acid (H<sub>2</sub>CY). The structures of several alkali metal salts<sup>6</sup> of CY and a cobalt–CY coordination polymer<sup>7</sup> have been reported, all containing the *cis* isomer; these materials were prepared at room temperature. By contrast, we recently described<sup>8</sup> hydrothermal reactions of manganese and cobalt salts with the *cis*-dicarboxylic acid that yielded only products containing the *trans*-acid, indicating that an isomerization of the organic component took place during the reactions. The driving force for this behavior was not clear. We have now studied the reaction of ZnO with H<sub>2</sub>CY at different temperatures and obtained products with both the *cis* and the *trans* ligands. On the basis of our experimental observations and *ab initio* calculations, we have attempted to rationalise the kinetic and thermodynamic factors that control the formation of the various products under different conditions.

Hydrothermal reactions† led to single crystals of three new zinc 1,2-dicarboxylates: Zn(C<sub>8</sub>H<sub>8</sub>O<sub>4</sub>)·2H<sub>2</sub>O, **1**, a dihydrate that forms at temperatures <100 °C, and two anhydrous polymorphs, α-Zn(C<sub>8</sub>H<sub>8</sub>O<sub>4</sub>), **2**, and β-Zn(C<sub>8</sub>H<sub>8</sub>O<sub>4</sub>), **3**, which were prepared at 150 °C. The β polymorph is the dominant product at higher temperatures, especially at longer reaction times. Varying the reaction conditions did not reveal any further phases.

The crystal structure<sup>9</sup> of **1** shows an unusual Zn<sup>2+</sup> coordination geometry (Fig. 1). There are four short Zn–O bonds (one to O5, a water O atom) with typical<sup>10</sup> bond lengths of 1.9409 (13)–2.0287 (12) Å and two much longer bonds, with Zn1–O1 = 2.5595 (12) and Zn1–O4b = 2.8445 (12) Å (see Figure captions for symmetry codes). These long bonds arise from bidentate –CO<sub>2</sub> moieties that are also linked to Zn by short bonds. The bond angles for the short Zn–O bonds correspond to distorted tetrahedral geometry [87.99 (5)–124.06 (5)°], but when the long bonds are also considered, no simple polyhedral shape results. An alternative description<sup>11</sup> is a “double-capped tetrahedron,” with the long Zn1–O1 and Zn1–O4b bonds protruding through the tetrahedral face described by O2, O3b and O5. The CY dianion in **1** is clearly the starting *cis* isomer, with the C1 carboxylate group equatorial and the C8 group axial with respect to the half-chair cyclohexene ring [torsion angle C8–C7–C2–H2 = 177°]. The second water molecule, O6, does not coordinate to the zinc but is located in the channels of the structure. Both water molecules participate in two O–H···O hydrogen bonds each. The crystal packing for **1** results in a two-dimensional coordination polymer with the zinc cations linked into *bc*-plane sheets by the CY dianions. The pendant organic groups interact with their neighbours in adjacent sheets by van der Waals forces (Fig. 2).

Compound **2** contains<sup>12</sup> two zinc cations and two CY dianions in the asymmetric unit (Fig. 3). Again, the zinc coordination is unusual: Zn1 has four close neighbours [Zn–O = 1.957 (3)–2.038 (3) Å] and a fifth O atom in its coordination sphere some 2.488 (4) Å distant. This ZnO<sub>5</sub> polyhedron could be described as a “singly capped tetrahedron”, with the long Zn1–O1 bond roughly protruding through the tetrahedral face defined by O2, O4b and

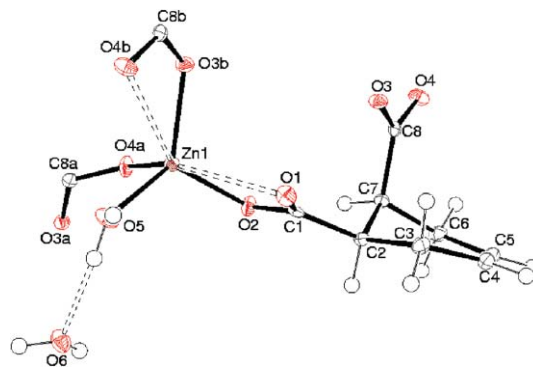


Fig. 1 Fragment of **1** showing the bicapped tetrahedron surrounding Zn. Symmetry codes: (a)  $-x, \frac{1}{2} + y, \frac{1}{2} - z$ , (b)  $-x, -y, -z$ . Ellipsoids shown at 50% displacement with arbitrary spheres for the hydrogen atoms.

<sup>a</sup>Materials Research Laboratory, University of California, Santa Barbara, CA 93106, USA. E-mail: cheetham@mrl.ucsb.edu

<sup>b</sup>Department of Chemistry, University of Aberdeen, Meston Walk, Aberdeen, AB24 3UE, Scotland

<sup>c</sup>Davy Faraday Research Laboratory, Royal Institution of Great Britain, 21 Albemarle Street, London, UK W1S 4BS

<sup>d</sup>Department of Chemistry and Biochemistry, University of California, Santa Barbara, CA 93106, USA

<sup>e</sup>Chemistry and Physics of Materials Unit, Jawaharlal Nehru Centre for Advanced Scientific Research, Jakkur, PO Bangalore, India-560064

† Electronic supplementary information (ESI) available: X-ray structural data for **1**, **2**, and **3** in cif format. See DOI: 10.1039/b603512d

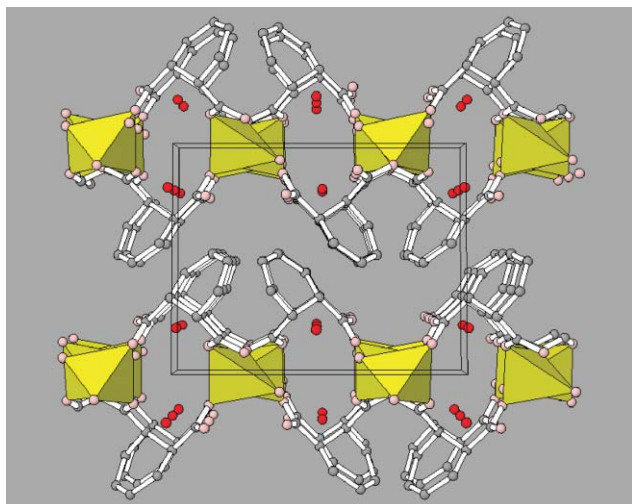


**Fig. 2** Polyhedral plot of **1** with  $\text{ZnO}_4$  tetrahedra shown in yellow, C atoms grey, coordinated O pink, non-coordinated water O red.

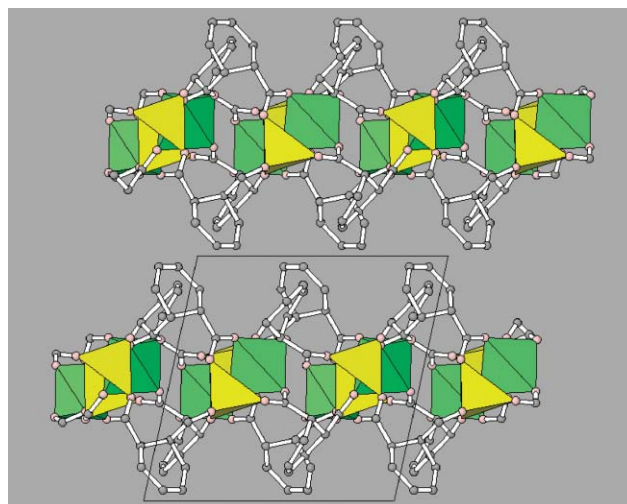


**Fig. 4** Polyhedral plot of the structure of **2**. Colours as Fig. 2 with the  $\text{ZnO}_5$  polyhedron coloured green.

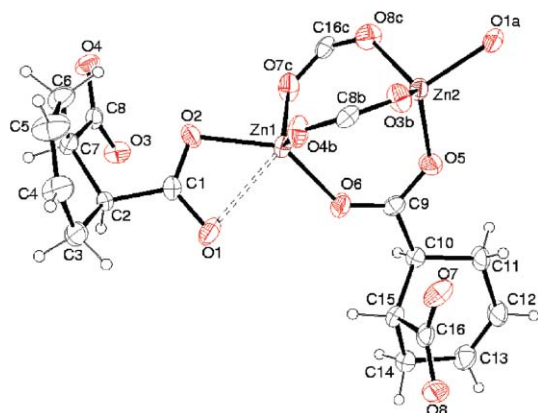


**Fig. 3** View of the atomic connectivity in **2**. Note how the Zn centres are bridged by three carboxylates (C atoms C9, C8b and C16c). Symmetry codes: (a)  $1 - x, y - 1/2, 1/2 - z$ ; (b)  $x, 1/2 - y, z - 1/2$ ; (c)  $x, 1/2 - y; z + 1/2$ .

O6. Zn2 is unambiguously tetrahedral, with four Zn–O bonds in the narrow range 1.924 (3)–1.943 (3) Å; the next nearest O atom is over 3.2 Å away. The CY dianions in **2** are both in their starting *cis* isomeric forms with C8/O3/O4 equatorial and C1/O1/O2 axial for the first molecule [C1–C2–C7–H7 = 172°] and C9/O5/O6 equatorial and C16/O7/O8 axial for the second [C16–C15–C10–H10 = 175°]. The structure of **2** again comprises a two-dimensional coordination polymer, with the Zn polyhedra bridged by the CY dianions (Fig. 4). Again, the pendant organic groups lie between the inorganic layers.

Phase **3** is isomorphous<sup>13</sup> with  $\text{Co}(\text{C}_8\text{H}_8\text{O}_4)^8$  and contains one  $\text{Zn}^{2+}$  cation and one CY dianion in the asymmetric unit. The coordination of Zn1 is significantly distorted tetrahedral, with Zn–O distances ranging from 1.914 (2) to 1.968 (2) Å and O–Zn–O angles from 99.10 (11) to 129.25 (12)°. In **3**, the CY dianion has isomerized to its *trans* form and both carboxylate moieties take up equatorial orientations with respect to the ring. The H3–C3–C4–H4 and C1–C3–C4–C2 torsion angles are 177 and 56.3 (4)°, respectively. As described earlier, **3** adopts a two-dimensional structure consisting of arrays of  $\text{ZnO}_4$  tetrahedra bridged into an

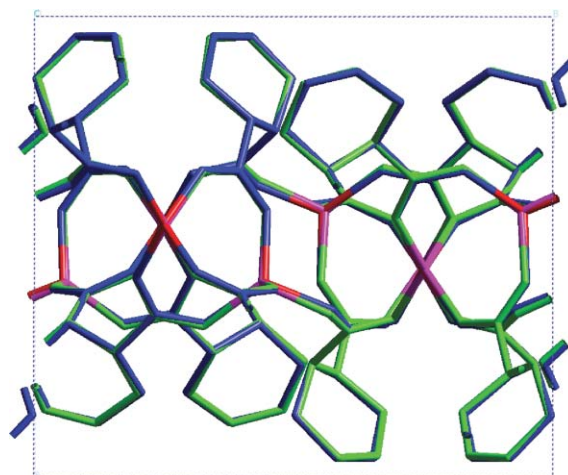


**Fig. 5** Comparison of experimental and DFT-relaxed *cis* structure, **2**. Hydrogen atoms have been omitted for clarity. Blue framework corresponds to the experimental *cis* structure, where the zinc atoms are highlighted in red. Relaxed structure shown in green where zinc atoms are shown in pink.

infinite sheet by way of the CY moieties. As seen in **1** and **2**, the pendant organic groups interact by van der Waals forces.

In order to obtain greater insight into the relative importance of kinetic *versus* thermodynamic factors during the syntheses of **1**, **2** and **3**, calculations of their relative total energies were carried out using first principle calculations, with the aim of understanding the influence of water and the ligand conformation (*cis* or *trans*) on the energetics of the different structures. The second goal was to identify the driving forces that lead to the formation of one structure rather than another as the reaction conditions are changed. In the absence of validated force fields for hybrid materials, plane wave based density functional theory (DFT) has proved to be efficient in addressing the energetics and structures of hybrid compounds.<sup>14</sup> Calculations were performed with CASTEP,<sup>15</sup> where a PBE exchange correlation function was used within the GGA approximation, with a kinetic energy cut-off of

340 eV. In each case, the energies were minimized by geometry optimization at constant volume (to minimise calculation artifacts due to imprecise sampling of dispersion forces) starting from the experimental structures and using the observed lattice parameters and symmetry. The energy-minimized structures are in very good agreement with the experimental ones, confirming the finding of recent work<sup>14</sup> that showed equally good agreement for a different family of hybrid materials (see Fig. 5).

The energies of the three hybrid structures normalized per zinc atom are as follows (with the corresponding densities in parentheses): **1**  $-5786.923$  eV ( $1.80$  g cm<sup>-3</sup>); **2**  $-4845.277$  eV ( $1.74$  g cm<sup>-3</sup>); **3**  $-4845.417$  eV ( $1.85$  g cm<sup>-3</sup>). Taking into account the energy of two water molecules ( $-940.522$  eV), the *cis*-dihydrate, **1**, is more stable than the *cis*-anhydrous phase, **2**, by  $\sim 1.12$  eV, or  $108$  kJ mol<sup>-1</sup>. Since the water is lost into solution under hydrothermal conditions, rather than into the gas phase, the internal energy change,  $\Delta E$ , for the reaction:



is approximately  $+27$  kJ mol<sup>-1</sup> (the heat of vaporization of two water molecules is  $81.2$  kJ mol<sup>-1</sup>). The calculations therefore show that the dehydration reaction is endothermic, indicating that the *cis*-dihydrate phase, **1**, should be more stable at lower temperatures, as observed. The formation of the anhydrous phase at the higher reaction temperatures can be rationalized in terms of the increase in configurational entropy associated with the release of water into solution in this reaction. In the light of these results, and given that dehydration reactions in a wide range of chemical systems occur on raising the temperature, it seems clear that the syntheses of **1** and **2** proceed under thermodynamic rather than kinetic control.

Turning now to the relative energies of the anhydrous *cis*- and *trans*-polymorphs, **2** and **3**, we find that **3** is more stable by  $0.14$  eV, *i.e.* approximately  $13.5$  kJ mol<sup>-1</sup>. This finding is consistent with its more dense structure ( $\sim 6\%$ ) and indicates that its formation is again thermodynamically driven. The other factor that is important here is that the *cis*- parent acid transforms under the higher temperature reaction conditions and with longer reaction times to the more stable *trans*-acid. In previous work, the *cis*-products have only been found at lower temperatures.<sup>7,8</sup> In the present work, we were fortunate on just one occasion to obtain crystals of the anhydrous *cis*-polymorph, **2**. Clearly, however, the kinetics do play a role in that there is a delicate balance at higher temperatures between the rate of isomerization of the acid and the rate of formation of the hybrid products.

The most striking finding from the present work is that our reactions appear to proceed primarily under local thermodynamic control. This might seem unusual by comparison with the aluminosilicate zeolite world, where hydrothermal reactions normally proceed under kinetic control, but it is consistent with our recent high throughput study of phase formation in cobalt succinates<sup>5</sup> and the observations of Attfield *et al.* on metal diphosphonates.<sup>14</sup> It remains to be seen whether such control is a general feature of hybrid material synthesis, or varies from one system to the next, depending on the rates of the metal–ligand exchange reactions.

## Notes and references

‡ The following reagents were used for the syntheses, as received: (i) zinc oxide (ZnO, Aldrich, 99+ %), (ii) 4-*cis*-cyclohexene-1,2-dicarboxylic acid (C<sub>8</sub>H<sub>10</sub>O<sub>4</sub>; H<sub>2</sub>CY, Acros Organics, 98%) and (iii) ethylene glycol (EG, Fisher Chemicals, 99+ %). A typical reaction involved the reagents H<sub>2</sub>O : ZnO : H<sub>2</sub>CY : EG in the molar ratios 420 : 1 : 1 : 24. ZnO, H<sub>2</sub>CY and EG were added sequentially to deionized water in 23 mL Teflon liners and stirred mechanically for 10 min. The opaque mixtures were then sealed in autoclaves and heated at temperatures between 60 and 150 °C for 48 hours. The initial pH was  $\sim 5.7$  and the final pH was in the range 4.1–5.2. The resultant products were suction-filtered, washed with deionized water, and dried in air at room temperature.

- C. N. R. Rao, S. Natarajan and R. Vaidyanathan, *Angew. Chem., Int. Ed.*, 2004, **43**, 1466.
- (a) O. M. Yaghi, M. O'Keefe, N. W. Ockwig, H. K. Chae, M. Eddaoudi and J. Kim, *Nature*, 2003, **423**, 705; (b) G. Férey, C. Mellot-Draznieks, C. Serre, F. Millange, J. Dutour, S. Surlblé and I. Margiolaki, *Science*, 2005, **309**, 2040.
- (a) B. Chen, S. S.-Y. Chui, S. M. F. Lo, J. P. H. Charmant, A. G. Orpen and I. D. Williams, *Science*, 1999, **283**, 1148–1150; (b) G. Férey, C. Serre, C. Mellot-Draznieks, F. Millange, S. Surlblé, J. Dutour and I. Margiolaki, *Angew. Chem., Int. Ed.*, 2004, **43**, 6296.
- (a) P. M. Forster and A. K. Cheetham, *Angew. Chem., Int. Ed.*, 2002, **41**, 457; (b) N. Guillou, C. Livage and G. Férey, *Angew. Chem., Int. Ed.*, 2003, **42**, 5314.
- (a) P. M. Forster, A. R. Burbank, C. Livage, G. Férey and A. K. Cheetham, *Chem. Commun.*, 2004, 368; (b) P. M. Forster, N. Stock and A. K. Cheetham, *Angew. Chem., Int. Ed.*, 2005, **44**, 7608.
- S. A. Kim and H. Küppers, *Z. Kristallogr.*, 1994, **209**, 789; S. A. Kim, *Acta Crystallogr., Sect. C: Cryst. Struct. Commun.*, 1995, **C51**, 1486.
- B. M. Ramirez, W. O. Velásquez and G. Díaz de Delgado, submitted for publication.
- D.-S. Kim, P. M. Forster, G. Diaz de Delgado and A. K. Cheetham, *Dalton Trans.*, 2004, 3365.
- Crystal data: 1*, Zn(C<sub>8</sub>H<sub>8</sub>O<sub>4</sub>)·2H<sub>2</sub>O, *M<sub>r</sub>* = 269.55, monoclinic, *P2<sub>1</sub>/c* (No. 14), *a* = 9.7790 (2) Å, *b* = 12.0260 (4) Å, *c* = 8.5260 (3) Å,  $\beta$  = 103.9436 (17)°, *V* = 973.13 (5) Å<sup>3</sup>, *Z* = 4,  $\mu$  = 2.53 mm<sup>-1</sup>,  $\rho_{\text{calc}}$  = 1.840 Mg m<sup>-3</sup>, *F*(000) = 552, *R*(*F*) = 0.026, *wR*(*F*<sup>2</sup>) = 0.052. Nonius KappaCCD diffractometer, Mo *K* $\alpha$  radiation,  $\lambda$  = 0.71073 Å, *T* = 120 K, 10666 reflections scanned ( $2\theta_{\text{max}}$  = 55°), 2228 unique (*R*<sub>int</sub> = 0.025). Water H atoms were located in difference maps and their positions were freely refined with *U*<sub>iso</sub>(H) = 1.2*U*<sub>eq</sub>(O). Carbon-bound H atoms were geometrically placed and refined as riding with *U*<sub>iso</sub>(H) = 1.2*U*<sub>eq</sub>(C). CCDC 298857. For crystallographic data in CIF or other electronic format see DOI: 10.1039/b603512d.
- I. Macdonald and W. T. A. Harrison, *Inorg. Chem.*, 2002, **41**, 6184.
- M. J. Johnston and W. T. A. Harrison, *Inorg. Chem.*, 2001, **40**, 6578.
- Crystal data: 2*,  $\alpha$ -Zn(C<sub>8</sub>H<sub>8</sub>O<sub>4</sub>), *M<sub>r</sub>* = 233.52, monoclinic, *P2<sub>1</sub>/c* (No. 14), *a* = 11.8544 (14) Å, *b* = 13.0110 (13) Å, *c* = 11.8523 (13) Å,  $\beta$  = 102.379 (2)°, *V* = 1785.6 (3) Å<sup>3</sup>, *Z* = 8,  $\mu$  = 2.73 mm<sup>-1</sup>,  $\rho_{\text{calc}}$  = 1.737 Mg m<sup>-3</sup>, *F*(000) = 552, *R*(*F*) = 0.039, *wR*(*F*<sup>2</sup>) = 0.095. Bruker SMART CCD diffractometer, Mo *K* $\alpha$  radiation,  $\lambda$  = 0.71073 Å, *T* = 293 K, 8257 reflections scanned ( $2\theta_{\text{max}}$  = 49°), 3017 unique (*R*<sub>int</sub> = 0.050). All H atoms were geometrically placed and refined as riding with *U*<sub>iso</sub>(H) = 1.2*U*<sub>eq</sub>(C). CCDC 298858. For crystallographic data in CIF or other electronic format see DOI: 10.1039/b603512d.
- Crystal data: 3*,  $\beta$ -Zn(C<sub>8</sub>H<sub>8</sub>O<sub>4</sub>), *M<sub>r</sub>* = 233.52, triclinic, *P* $\bar{1}$  (No. 2), *a* = 4.8606 (4) Å, *b* = 6.7240 (5) Å, *c* = 13.1788 (11) Å,  $\alpha$  = 98.071 (1)°,  $\beta$  = 98.236 (1)°,  $\gamma$  = 95.585 (1)°, *V* = 419.01 (6) Å<sup>3</sup>, *Z* = 2,  $\mu$  = 2.91 mm<sup>-1</sup>,  $\rho_{\text{calc}}$  = 1.851 Mg m<sup>-3</sup>, *F*(000) = 236, *R*(*F*) = 0.034, *wR*(*F*<sup>2</sup>) = 0.093. Bruker SMART CCD diffractometer, Mo *K* $\alpha$  radiation,  $\lambda$  = 0.71073 Å, *T* = 293 K, 3229 reflections scanned ( $2\theta_{\text{max}}$  = 52°), 1595 unique (*R*<sub>int</sub> = 0.020). All H atoms were geometrically placed and refined as riding with *U*<sub>iso</sub>(H) = 1.2*U*<sub>eq</sub>(C). CCDC 298856. For crystallographic data in CIF or other electronic format see DOI: 10.1039/b603512d.
- H. G. Harvey, B. Slater and M. P. Attfield, *Chem.–Eur. J.*, 2004, **10**, 3270.
- M. D. Segall, P. J. D. Lindan, M. J. Probert, C. J. Pickard, P. J. Hasnip, S. J. Clarke and M. C. Payne, *J. Phys.: Condens. Matter*, 2002, **14**, 2717.